

# Cobalt Vanadium Heterointerface Modulated Co<sub>2</sub>P/VP Heterostructure Electrocatalyst for Robust Water Splitting

Purna Prasad Dhakal\*, Ganesh Bhandari\*, Hoang Tuan Nguyen\*, Duy Thanh Tran\*,  
Nam Hoon Kim\*†, Joong Hee Lee\*,\*\*†

**ABSTRACT:** The rational synthesis of efficient transitional metal phosphides (TMPs) could revolutionize green hydrogen production via water splitting. Hydrogen, with the highest energy density among fuels, stands out as an excellent alternative to address environmental issues and ensure sustainable future energy generation. However, the limited availability of state-of-the-art electrocatalysts like Pt/C and RuO<sub>2</sub>, used for the hydrogen evolution reaction (HER) and oxygen evolution reaction (OER), necessitates the development of cost-effective and non-noble electrocatalysts for green hydrogen production. In this context, we present a novel heterointerface-modulated heterostructure design comprising ultrathin nanosheets of a 3D Co<sub>2</sub>P/VP heterostructure on a conductive nickel foam substrate. This heterostructure demonstrates remarkably low overpotentials of 96 mV for HER and 237 mV for OER at 10 mA cm<sup>-2</sup>. The material's robust electrochemical kinetics are further evidenced by low Tafel slopes of 68.28 mV dec<sup>-1</sup> and 116.54 mV dec<sup>-1</sup>, respectively.

**Key Words:** Phosphides, HER, OER, Heterostructure, Water splitting

## 1. INTRODUCTION

The growing demand for renewable and clean energy is becoming increasingly critical due to the rapid depletion of fossil fuels and the environmental pollution they cause. As petroleum reserves dwindle, the world faces a potential energy crisis of unprecedented scale. Therefore, developing sustainable energy alternatives is imperative to meet future energy needs. In this context, clean hydrogen production through overall water splitting stands out as one of the best alternatives to address future energy requirements [1]. Nevertheless, the zero-carbon goal via the exploration of clean energy is a desperate concern. To the context, production of hydrogen via the electrolysis may be the best sustainable solution. More precisely, the water splitting occurs via a simultaneous process of hydrogen evolution reaction (HER) at cathode and oxygen evolution reaction (OER) at anode [2]. However, the sluggish kinetics of complex four electron transfer mechanism in the

electrochemical OER process is one of the bottlenecks. Moreover, the commercial electrode materials for the HER i.e., (Pt-based) and OER (Ru-based) are expensive with the limited reservoir, hinders the widespread application for the overall water splitting. So, the electrocatalyst in the adequate amount and cheap has the great potential for the generation of clean hydrogen. In this context, numerous transition metal-based electrocatalysts have been fabricated, including layered double hydroxides (LDH) and transition metal chalcogenides (TMS) such as phosphides, sulfides, and tellurides. These materials are favored due to their facile synthesis methods and cost-effectiveness [3,4]. More specifically, nickel and vanadium-based chalcogenides have significant potential for the hydrogen evolution reaction (HER), oxygen evolution reaction (OER), and overall water splitting (OWS). This is due to the optimal properties of first-row transition metals, such as variable oxidation states, a tendency for complex formation, and excellent electrical conductivity [5,6]. Among transition metal

Received 1 June 2024, received in revised form 12 June 2024, accepted 6 August 2024

\*Department of Nano Convergence Engineering, Jeonbuk National University, Jeonju 54896, Korea

\*\*Carbon Composite Research Center, Department of Polymer-Nano Science and Technology, Jeonbuk National University, Jeonju 54896, Korea

†Corresponding authors, Prof. Nam Hoon Kim (E-mail: [nhk@jbnu.ac.kr](mailto:nhk@jbnu.ac.kr)) and Prof. Joong Hee Lee (E-mail: [jhl@jbnu.ac.kr](mailto:jhl@jbnu.ac.kr))

chalcogenides (TMS), nickel and vanadium-based phosphides exhibit a strong quantum size effect, outstanding electrical conductivity due to their shallow valence band, low toxicity, and ease of synthesis [7]. In this regard, both monometallic and polymetallic metal phosphides have been fabricated. However, single metallic tellurides exhibit relatively low electrochemical performance. Introducing more than one transition metal in functionally modified transition metal phosphides (TMPs) can significantly enhance their HER and OER potential [2,8]. In particular, synergistic activities across the multimetallic moieties are a key factor in enhancing electrochemical performance.

Herein, we have facilely synthesized a bimetallic cobalt vanadium phosphide (Co<sub>2</sub>P/VP) heterointerface-modulated structure through the rational manipulation of its electronic structure. The as-synthesized electrocatalyst demonstrates outstanding HER and OER performance in a 1.0 M alkaline electrolyte at 25°C, with overpotentials of 96 mV and 237 mV at current densities of 10 mA cm<sup>-2</sup>, respectively. The remarkable electrochemical activity of the synthesized Co<sub>2</sub>P/VP is attributed to the synergism between the metallic configurations and the tailored electronic structure.

## 2. EXPERIMENTAL

### 2.1 Chemicals and instruments

Cobalt (II) nitrate hexahydrate (Co(NO<sub>3</sub>)<sub>2</sub>·6H<sub>2</sub>O; ≥99.0%), sodium orthovanadate dihydrate (Na<sub>3</sub>VO<sub>4</sub>·2H<sub>2</sub>O; ≥99.0%), ammonium fluoride (NH<sub>4</sub>F; ≥99.0%), urea (NH<sub>2</sub>CONH<sub>2</sub>; ≥99.0%), sodium phosphite monohydrate (NaH<sub>2</sub>PO<sub>2</sub>·H<sub>2</sub>O ≥99.0%) ruthenium (IV) oxide (99.9% trace metal basis), Pt/C (10 wt.% loading) were purchased from Sigma-Aldrich and used without further purification. Numbers of modern and advanced instruments were used for the synthesis of materials and their characterizations. For the morphological inspection, field emission scanning electron microscopy (Marker: Supra 40 VP instrument Zeiss Co., Germany) was used. For the crystallographic characterization, X-ray diffraction meter (Marker: D/Max 2500 V/PC; Rigaku Co., Japan) was used at the Center for University-Wide Research Facilities (CURF), Jeonbuk National University (Republic of Korea). Cu target Kα X-ray (λ = 0.154 nm) was used as the source of X-ray. X-ray photoelectron spectrometry (marker: VG ESCALAB 220i, Thermo Fischer, UK) was used in the Jeonju center of KBSI (Republic of Korea). CHI660 electrochemical workstation (CH Instruments, Inc., USA) was used for the electrochemical measurements of as-prepared materials.

### 2.2 Preparation of cobalt vanadium layered double hydroxide (CoV-LDH)

The 2D CoV-LDH nanosheets were synthesized on nickel foam via a one-step hydrothermal method. In detail, 0.57 g cobalt nitrate hexahydrate, 0.22 g sodium orthovanadate dihy-

drate, 0.30 g urea, and 0.09 g ammonium fluoride were dissolved into 60 mL deionized water following continuous stirring for 15 min at room temperature to make a clear homogenous solution. Then a clean NF of size (2 × 5 cm<sup>2</sup>) was placed inside a 100 mL teflon-lined stainless-steel autoclave. After that, all 60 mL solution was poured followed by self-cooling to room temperature to complete the reaction and the formation of CoV-LDH. After the completion of reaction, the nickel foam was taken out and washed with deionized (DI) water followed by ethanol several times and dried at 60°C under vacuum for 12 h.

### 2.3 Preparation of cobalt vanadium phosphide (Co<sub>2</sub>P/VP) heterostructure

The CoV-LDH loaded nickel foam was directly transformed to vanadium phosphide (Co<sub>2</sub>P/VP) heterostructure via simultaneous phosphorization process by a one-step controlled chemical vapor deposition (CVD) method. In detail, the CoV-LDH loaded NF was then placed in the upstream and 0.25 g NaH<sub>2</sub>PO<sub>2</sub>·H<sub>2</sub>O in the downstream side of the CVD boat, which was kept inside the glass tube of the CVD furnace. Next, the reaction was started with continuous flow of argon (Ar) gas with the ramping rate of 100 sscm at 400°C for 1 h. After the completion of the phosphorization, the Co<sub>2</sub>P/VP was washed with ethanol and kept in vacuum for 6 h to dry at 60°C. The mass loading of the Co<sub>2</sub>P/VP in nickel foam was determined as 4.1 mg cm<sup>-2</sup>.

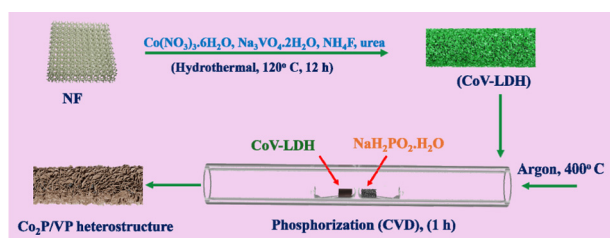
### 2.4 Electrochemical characterization

The electrochemical performance of the prepared samples was analyzed using a CHI660D workstation. Linear sweep voltammetry (LSV) was evaluated on these samples using a three-electrode setup containing Ag/AgCl electrode as reference electrode, graphite rod as counter electrode, and nickel foam loaded with Co<sub>2</sub>P/VP (1 × 1 cm<sup>2</sup>) served as the binder free working electrode. 1.0 M KOH was used as electrolyte. The linear sweep voltammetry (LSV) was measured at the scan rate of 2 mV s<sup>-1</sup>, employing 100% iR compensation.

## 3. RESULTS AND DISCUSSION

The synthesis of CoV-LDH nanosheet arrays is achieved via hydrothermal approach. Herein, the ultrathin nanosheet was initially grown via facile hydrothermal approach at the optimum temperature at 12 h (details in the experimental section). Then the CoV-LDH was used as the sacrificial template for the post functionalization (phosphidation) by the controlled CVD method to synthesize Co<sub>2</sub>P/VP heterostructure as shown in Scheme 1.

Additionally, the phosphine gas produced from the sodium phosphide monohydrate at the operating temperature causes the solid-gas reaction to form the Co<sub>2</sub>P/VP [9] The ion exchange process between the (OH<sup>-</sup>) group of the LDH and



**Scheme 1.** Schematic representation of the synthesis details of  $\text{Co}_2\text{P/VP}$  electrocatalyst

the phosphide ion results in the formation of corresponding heterophasic bimetallic phosphide. The scanning electron microscopy (SEM) imagery shows the uniformly grown ultrathin nanosheet structure of the  $\text{Co}_2\text{P/VP}$  morphology. The elongation of same morphology shows no over agglomeration throughout the nickel foam, featuring towards the good performance (Fig X). Additionally, the FE-SEM elemental color mapping of the  $\text{Co}_2\text{P/VP}$  shows the presence of Co, V, and P, confirming the successful formation of the material (Fig. 1).

The crystalline structure and the formation of phases of the material was examined through the X-ray diffraction (XRD) examination (Fig. 2). The  $2\theta$  corresponding to the  $40.7^\circ$ ,  $43.2^\circ$ , and  $50.3^\circ$  are ascribed to the (1 2 1), (2 1 1), and (3 1 0) planes

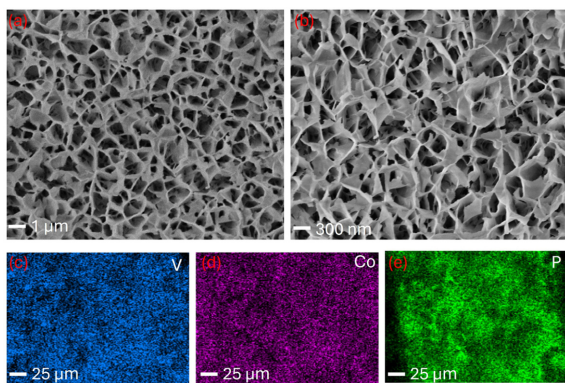


**Fig. 1.** FESEM images of (a-b)  $\text{Co}_2\text{P/VP}$  and (c-e) corresponding EDS color mapping of the  $\text{Co}_2\text{P/VP}$  electrocatalyst

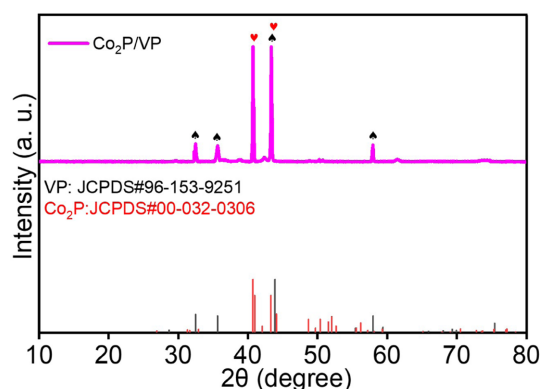


**Fig. 2.** XRD patterns of  $\text{Co}_2\text{P/VP}$  electrocatalyst

of  $\text{Co}_2\text{P}$ , respectively (PDF No. 00-032-0306) [10]. Similarly, the  $2\theta$  corresponding to the  $28.68^\circ$ ,  $32.48^\circ$ ,  $35.6^\circ$ ,  $43.14^\circ$ ,  $57.95^\circ$ , and  $75.43^\circ$  (002), (100), (101), (102), (110), and (202), are ascribed to the respectively of VP (JCPDS#96-153-9251). Overall, formation of the  $\text{Co}_2\text{P}$  and VP phases confirms the formation of  $\text{Co}_2\text{P/VP}$  heterostructure.

### 3.1 Electrochemical measurement of the materials

The electrochemical HER performance of the as-synthesized  $\text{Co}_2\text{P/VP}$  heterostructure material were evaluated in the typical three electrode system under room temperature using LSV measurement technique at  $2 \text{ mV s}^{-1}$  scan rate. The observations were made for CoV-LDH,  $\text{RuO}_2$ , and  $\text{Co}_2\text{P/VP}$  heterostructure. The  $\text{Co}_2\text{P/VP}$  electrocatalyst performs superior to the comparison electrode materials with the significantly low overpotential  $\eta$  of 96 mV at the current density of  $10 \text{ mA cm}^{-2}$ , which is close to the overpotential of Pt/C (52 mV) and significantly smaller than the CoV-LDH (131 mV) (Fig. 3a), proving the robustness of the  $\text{Co}_2\text{P/VP}$  toward HER. The robustness of the electrode material was measured by evaluating the Tafel slopes (Fig. 3b) [11]. The Tafel slope of the as-prepared  $\text{Co}_2\text{P/VP}$  heterostructure is  $(68.28 \text{ mV dec}^{-1})$ , showing the superiority over the comparison electrode materials like, CoV-LDH ( $110.21 \text{ mV dec}^{-1}$ ) and closed to the Pt/C ( $49.14 \text{ mV dec}^{-1}$ ). The significantly low Tafel slope indicates the robust kinetics of the material owing to the electronic modulation among the electronegative P atom of the entire

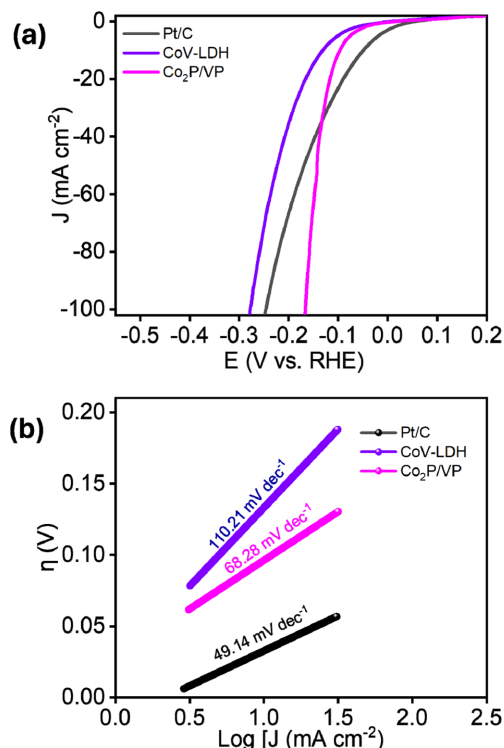


**Fig. 3.** (a)  $iR$ -corrected LSV plot, and (b) Tafel plots of the various as-synthesized electrocatalysts for alkaline HER

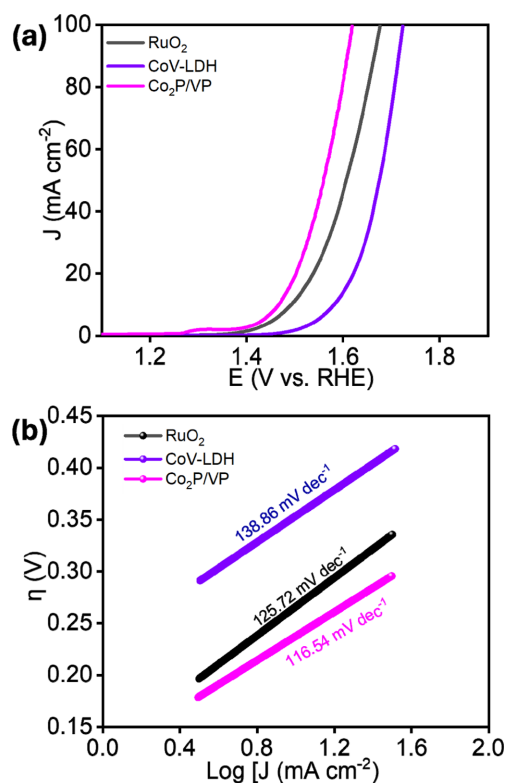


**Fig. 4.** (a) iR-corrected LSV plot, and (b) Tafel slopes of the various as-synthesized electrocatalysts for alkaline OER

bimetallic phosphide moiety, hastening the charge/mass transfer along the electrode-electrolyte interface.

The electrochemical OER Co<sub>2</sub>P/VP heterostructure material were evaluated in the identical condition of the three-electrode set up as in the case of HER. The OER performance of the as-synthesized Co<sub>2</sub>P/VP heterostructure, CoV-LDH, and commercial RuO<sub>2</sub> were evaluated through the LSV measurements (Fig. 4a). The results reveals that the Co<sub>2</sub>P/VP heterostructure has outstanding performance of lower overpotential  $\eta$  of 237 mV, which is superior to the benchmark RuO<sub>2</sub> (260 mV) and CoV-LDH (270 mV). The reaction kinetics of the electrode materials were through the Tafel plots after iR-compensation, which shows the lower value of Co<sub>2</sub>P/VP (116.54 mV dec<sup>-1</sup>) compared to the RuO<sub>2</sub> (125.72 mV dec<sup>-1</sup>), and CoV-LDH (138.6 mV dec<sup>-1</sup>) (Fig. 4b). The results clearly indicate that the heterointerface modulated structure could facilitates the reaction kinetics towards the OER performance. Overall, the as-synthesized Co<sub>2</sub>P/VP is efficient owing to the multiple functional moieties integrated within a composite, which rationally manipulate the electronic structure via the high spin metal cations with the more electronegative P atom within the bimetallic phosphide.

#### 4. CONCLUSIONS

In this research, we have successfully fabricated the het-

erointerface modulated Co<sub>2</sub>P/VP ultrathin nanosheets based heterostructure. This unique composite architecture promotes synergistic effect of bimetal-based phosphide moiety in the nickel foam support. The outstanding performance of the material occurs via enhancement of physiochemical properties by creating the multiple active sites, outstanding stability, and hydrophilicity, offers robust HER and OER performances in an alkaline condition with lower overpotential of 96 mV and 260 mV towards HER and OER, respectively at the current density of 10 mA cm<sup>-2</sup>. This research offers a novel alternative of material engineering through the facile fabrication of bifunctional electrocatalyst for the overall water splitting.

#### REFERENCES

- Wang, Y., Lv, H., Sun, L., Jia, F., and Liu, B., "Ordered Mesoporous Intermetallic Trimetals for Efficient and pH-Universal Hydrogen Evolution Electrocatalysis," *Advanced Energy Materials*, Vol. 12, 2022, pp. 2201478.
- Pan, U.N., Paudel, D.R., Kumar Das, A., Singh, T.I., Kim, N.H., and Lee, J.H., "Ni-nanoclusters Hybridized 1T-Mn-VTe<sub>2</sub> Mesoporous Nanosheets for Ultra-low Potential Water Splitting," *Applied Catalysis B: Environmental*, Vol. 301, 2022, pp. 120780.
- Zhou, L., Jiang, S., Liu, Y., Shao, M., Wei, M., and Duan, X., "Ultrathin CoNiP@Layered Double Hydroxides Core-Shell Nanosheets Arrays for Largely Enhanced Overall Water Splitting," *ACS Applied Energy Materials*, Vol. 1, 2018, pp. 623-631.
- Zeng, L., Sun, K., Wang, X., Liu, Y., Pan, Y., Liu, Z., Cao, D., Song, Y., Liu, S., and Liu, C., "Three-Dimensional-networked Ni<sub>2</sub>P/Ni<sub>3</sub>S<sub>2</sub> Heteronanoflake Arrays for Highly Enhanced Electrochemical Overall-water-splitting Activity," *Nano Energy*, Vol. 51, 2018, pp. 26-36.
- Zhu, H., Zhang, J., Yanzhang, R., Du, M., Wang, Q., Gao, G., Wu, J., Wu, G., Zhang, M., Yao, J., Zhang, X., "When, Cubic Cobalt Sulfide Meets Layered Molybdenum Disulfide: A Core-Shell System Toward Synergetic Electrocatalytic Water Splitting," *Advanced Materials*, Vol. 27, 2015, pp. 4752-4759.
- Zeng, J., Zhang, L., Zhou, Q., Liao, L., Qi, Y., Zhou, H., Li, D., Cai, F., Wang, H., Tang, D., and Yu, F., "Boosting Alkaline Hydrogen and Oxygen Evolution Kinetic Process of Tungsten Disulfide-Based Heterostructures by Multi-Site Engineering," *Small*, Vol. 18, 2022, pp. 2104624.
- Hoa, V.H., Tran, D.T., Le, H.T., Kim, N.H., and Lee, J.H., "Hierarchically Porous Nickel-cobalt Phosphide Nanoneedle Arrays Loaded Micro-carbon Spheres as an Advanced Electrocatalyst for Overall Water Splitting Application," *Applied Catalysis B: Environmental*, Vol. 253, 2019, pp. 235-245.
- Shi, J., Huan, Y., Zhao, X., Yang, P., Hong, M., Xie, C., Pennycook, S., and Zhang, Y., "Two-Dimensional Metallic Vanadium Ditelluride as a High-Performance Electrode Material," *ACS Nano*, Vol. 15, 2021, pp. 1858-1868.
- Kandel, M.R., Pan, U.N., Dhakal, P.P., Ghising, R.B., Nguyen, T.T., Zhao, J., Kim, N.H., and Lee, J.H., "Unique Heterointerface Engineering of Ni<sub>2</sub>P-MnP Nanosheets Coupled Co<sub>2</sub>P Nano-

- flowers as Hierarchical Dual-functional Electrocatalyst for Highly Proficient Overall Water-splitting,” *Applied Catalysis B: Environmental*, Vol. 331, 2023, pp. 122680.
10. Dhakal, P.P., Pan, U.N., Kandel, M.R., Ghising, R.B., Nguyen, T.H., Dinh, V.A., Kim, N.H., and Lee, J.H., “Cobalt Phosphide Integrated Manganese-doped Metallic 1T-vanadium Disulfide: Unveiling a 2D-2D Tangled 3D Heterostructure for Robust Water Splitting,” *Chemical Engineering Journal*, Vol. 473, 2023, pp. 14532.
  11. Dhakal, P.P., Pan, U.N., Paudel, D.R., Kandel, M.R., Kim, N.H., and Lee, J.H., “Cobalt-manganese Sulfide Hybridized Fe-doped 1T-Vanadium Disulfide 3D-Hierarchical Core-shell Nanorods for Extreme Low Potential Overall Water-splitting,” *Materials Today Nano*, Vol. 20, 2022, pp. 100272.